

**P. K. Venu Vinod**

Asst. Professor,  
Regional Engineering College,  
Warangal, India

**Waishing Lau**

Senior Lecturer,  
Hongkong Polytechnic

**G. Barrow**

Senior Lecturer,  
University of Manchester,  
Institute of Science and Technology,  
Manchester, U.K.

## On a New Model of Oblique Cutting

### Introduction

Today, there exist a variety of models for orthogonal cutting. These cover a wide range of concepts with the simple shear plane models at one end and the complex slip line models at the other end. Each model emphasises a particular aspect at the cost of others. Yet, it is the existence of this variety which enables us to have an understanding of the totality of metal cutting though no single model is able to cover the totality.

The situation with oblique cutting is entirely different. With the exception of shear plane models [1, 2]<sup>1</sup> and others involving mean shear zone thickness [3] etc., no serious attempt has been made to extend other models of orthogonal cutting to problems of non-plane-strain cutting. Such extensions are, however, desirable since they would throw more light on aspects hitherto unexplored in oblique cutting. This will also test the model in a new environment and would throw greater light on its advantages and limitations.

This paper aims at extending to oblique cutting, a pseudo-slip line solution proposed by Connally and Rubenstein [4] for orthogonal cutting. After developing the model it is verified against the experimental data available in literature and the implications discussed.

### Connally and Rubenstein's Orthogonal Cutting Model

Fig. 1(a) shows the assumed bounds of the primary deformation zones. These bounds must obviously be slip lines. Consider a slip line close to the lower bound. For simplicity, let the transient curve joining

the unmachined surface to the chip surface be ignored. The slip line then meets the unmachined surface at 45 deg.  $OB$  is then the nominal shear plane used in Merchant's [1] analysis. The slip line is further assumed to be parallel to the cutting speed at the end it meets the cutting edge. This feature and the absence of the transient surface are valid flaws in the model.

The cutting forces contributed by chip formation can be estimated if the stress distribution on the slip surface are known. It is more attractive to consider a slip surface close to the lower boundary of shear zone, since the material there is still in the virgin state. The curvature of the lower bound surface is usually low. It is therefore permissible to replace the slip surface by two planes ( $S$  and  $L$ -planes) parallel to it at each end. The error involved in such a procedure would be low as far as the estimation of cutting forces is concerned. It would of course be undesirable to stretch the model to other aspects of machining like the determination of exact stress and strain distributions etc.

The stress distribution along the  $S$  and  $L$  planes may be estimated from the well known properties of slip lines. Integrating these stresses and taking appropriate components it is possible to estimate the cutting forces. Such estimations made by Connally and Rubenstein [4] agreed well with experimental observations. Rubenstein [5, 6] further used the theory to investigate other features of metal cutting with reasonable success. In these he used the length ' $l$ ' of the  $L$ -plane as a parameter similar in scope to the shear angle in conventional analysis.

### The New Oblique Cutting Model

On the basis of empirical evidence, it may be said that the primary effect of obliquity is to change the orientation of slip on the slip surfaces on the primary deformation zone. When one attempts at the extension of Connally and Rubenstein's model to oblique cutting, one is tempted to keep the  $S$  and  $L$ -planes as they are and introduce lateral slips. This is in line with Merchant's [1] approach where he in-

<sup>1</sup> Numbers in brackets designate References at end of paper.

Contributed by the Production Engineering Division and presented at the Winter Annual Meeting, Atlanta, Ga., November 27-December 2, 1977 of THE AMERICAN SOCIETY OF MECHANICAL ENGINEERS. Manuscript received at ASME Headquarters June 27, 1977. Paper No. 77-WA/PROD-6.

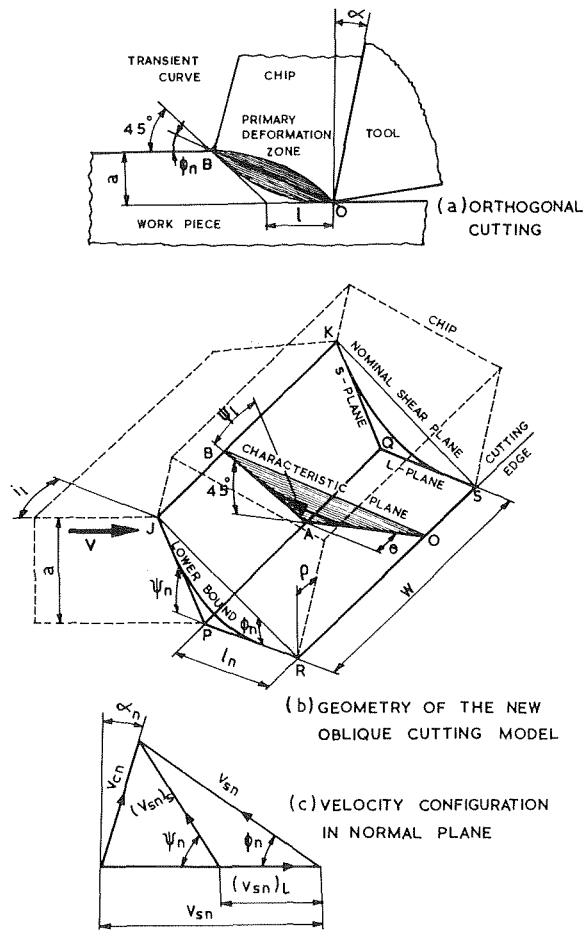


Fig. 1 The new oblique cutting model

troduced lateral slips on the conventional shear plane to take into account the effect of obliquity. However, this would mean that the actual slip lines are now inclined to the normal plane. If the *S* plane is kept inclined to the cutting plane at 45 deg, the slip lines would meet the free surface at an angle less than 45 deg. It is therefore necessary to change the orientation of *S*-plane accordingly.

Fig. 1(b) illustrates the basic features of the proposed model. *RS* is the cutting edge. Plane *RJKS* is the nominal shear plane. Curved surface *RJKS* is the slip surface under consideration. Planes *PJKQ* (*S*-plane) and *PQSR* (*L*-plane) are drawn tangential to surface *RJKS* at each end. The *S*-plane is inclined to the cutting plane at angle  $\psi_n$  whereas the *L*-plane is in it. *PQ* is the line of intersection of the *S* and *L*-planes.  $l_n$  is the length of *S*-plane.

Shear is assumed to take place on surface *RJKS* in the direction represented by curve *OB*. For simplicity it is assumed that *OB* is a plane curve perpendicular to the cutting plane.  $\theta$  is the angle made by this characteristic plane with the normal plane.  $\theta$  may thus be considered as the lateral shear angle in the *L*-plane.  $\psi_\ell$  is the corresponding angle in the *S*-plane. *AB* which is tangential to the orientation of shear in the *S*-plane should be at 45 deg to the cutting plane. From the geometry of Fig. 1(b) the following expressions can now be obtained.

$$\tan \psi_n = \sec \theta \text{ or cosec } \psi_n = (1 + \cos^2 \theta)^{1/2} \quad (1)$$

$$\sin \psi_\ell = \sin \theta / \sqrt{2} \quad (2)$$

and

$$l_n = a (\cos \phi_n - \cos \theta) \quad (3)$$

Where  $\phi_n$ , the nominal normal shear angle may be obtained from the chip compression ratio  $a_c/a$  from the following relationship.

$$\tan \phi_n = \frac{\cos \alpha_n}{a_c/a - \sin \alpha_n} \quad (4)$$

The areas  $A_S$  and  $A_L$  of the *S* and *L*-planes are given by

$$A_S = aw (1 + \cos^2 \theta)^{1/2} \quad (5)$$

and

### Nomenclature

$A_S, A_L$  = Areas of *S* and *L*-planes respectively

$i$  = Angle of inclination, complement of the angle between cutting speed and cutting edge vectors

$l, l_n$  = Length of *L* plane in orthogonal and oblique cutting respectively

$N_S, N_L$  = Normal forces on the *S* and *L*-planes respectively

$N_{Sn}, N_{Sy}$  = Normal and thrust components of  $N_S$  respectively

$S_S, S_L$  = Shear forces on the *S* and *L*-planes respectively

$S_{Sn}, S_{Sl}, S_{Sy}$  = Normal, lateral and thrust components respectively of  $S_S$

$S_{L_n}, S_{Ll}$  = Normal and lateral components of  $S_L$  respectively

$P_n, P_l, P_y$  = Normal, lateral and thrust components respectively of the cutting forces

$P_n', P_l', P_y'$  = Magnitudes of  $P_n, P_l$  and  $P_y$  contributed by chip formation, i.e., with the parasitic forces at the cutting edge and the tool flank eliminated

$V$  = Cutting speed

$V_s$  = Velocity of shear on Merchant's shear plane

$V_c$  = Velocity of chip

$V_n, V_l$  = Normal and lateral components of  $V$

$V_{sn}, V_{sl}$  = Normal and lateral components of  $V_s$

$V_{cn}, V_{cl}$  = Normal and lateral components of  $V_c$

$(V_{sn})_S, (V_{sn})_L$  = Contribution to  $V_{sn}$  by *S* and *L*-planes respectively

$(V_{sl})_S, (V_{sl})_L$  = Contributions to  $V$  by *S* and *L*-planes respectively

$V_t$  = Velocity of rotary motion of a rotary tool

$w$  = Length of cutting edge in engagement, width of cut

$\alpha_n$  = Rake angle measured in normal plane

$\phi_n$  = Shear angle measured in normal plane

$\psi_\ell$  = Angle between direction of shear on *S*-plane and trace of normal plane on *S*-plane

$\psi_n$  = Angle between the cutting plane and the *S*-plane

$\theta$  = Characteristic angle, angle between direction of shear on *L*-plane and normal to the cutting edge

$\theta_p$  = Value of  $\theta$  estimated from chip flow angle

$\rho$  = Chip flow angle, angle between the direction of chip flow and normal to the cutting edge measured on the rake surface

Cutting plane = Plane including the cutting edge and cutting speed vectors

Normal plane = Plane normal to the cutting plane

Characteristic plane = A plane normal to the cutting plane and assumed to be including the directions of shear on all the slip surfaces in the primary deformation zone

Normal component = A component of the given vector normal to the cutting edge

Lateral component = A component of the given vector parallel to the cutting edge

Thrust component = A component of the given vector in a direction normal to the machined surface

$$A_L = aw (\cot \phi_n - \cos \theta) \quad (6)$$

It may be noticed that angle  $\psi_n \geq 45$  deg. For orthogonal cutting  $\theta = 0$ ,  $\psi_n = 45$  deg as assumed in the orthogonal cutting model. As in the case of orthogonal cutting  $l_n$  may be interpreted as a parameter similar in scope to the shear angle but in the present case it also includes the effect of obliquity indirectly through  $\theta$ .

The  $S$ -plane extends upto the free surface. Therefore the normal and shear stresses on the plane are equal to the flow stress  $\tau_s$  of the work material. Multiplying these stresses with the area  $A_S$  of the plane the magnitudes of the shear force  $S_S$  and normal force  $N_S$  can be found. From the knowledge of angles  $\psi_n$  and  $\psi_l$  these forces can be divided into the normal ( $S_{Sn}$ ,  $N_{Sn}$ ), lateral ( $S_{Sl}$ ) and thrust ( $S_{Sy}$ ,  $N_{Sy}$ ) components. Plane  $L$  being a slip plane, the shear stresses on it is again  $\tau_s$ . But the mean normal stress 'p' on it is unknown. Multiplying these stresses with the area  $A_L$  of the plane, the shear ( $S_L$ ) and normal forces ( $N_L$ ) can be determined. These can be resolved further into the normal ( $S_{Ln}$ ), lateral ( $S_{L1}$ ) and thrust ( $N_L$ ) components. Cutting force components  $P_n'$ ,  $P_l'$  and  $P_y'$  may be obtained by summing up the appropriate components from the above.

The following expressions are obtained after simplification.

$$\begin{aligned} P_n' &= S_{Sn} + N_{Sn} + S_{L1} \\ &= \tau_s A_S \cos 45 \text{ deg} \cos \theta + \tau_s A_S \sin \psi_n + \tau_s A_L \cos \theta \\ &= \tau_s a w [1 + \cos \theta \left( \frac{1 + \cos^2 \theta}{2} \right)^{1/2} - \cos \theta + \cos \phi_n]. \end{aligned} \quad (7)$$

$$\begin{aligned} P_l' &= S_{Sl} + S_{L1} \\ &= \tau_s A_S \cos 45 \text{ deg} \sin \theta + \tau_s A_L \sin \theta \\ &= \tau_s a w \sin \theta \left[ \left( \frac{1 + \cos^2 \theta}{2} \right)^{1/2} - \cos \theta + \cot \phi_n \right] \end{aligned} \quad (8)$$

$$\begin{aligned} P_y' &= S_{Sy} + N_{Sy} + N_L \\ &= \tau_s A_S \sin 45 \text{ deg} + \tau_s A_S \cos \psi_n + p A_L \\ &= a w \left[ p (\cot \phi_n - \cos \theta) - \tau_s \cos \theta - \tau_s \left( \frac{1 + \cos^2 \theta}{2} \right)^{1/2} \right] \end{aligned} \quad (9)$$

An expression for parameter  $\theta$  may be obtained by dividing equation 7 with equation 8. Thus, in terms of force components  $P_n'$  and  $P_l'$  we have,

$$\begin{aligned} \cos \theta - \left( \frac{P_n'}{P_l'} \right) \sin \theta \\ + \left[ \left( \frac{1 + \cos^2 \theta}{2} \right)^{1/2} - \cos \theta + \cot \phi_n \right]^{-1} = 0 \end{aligned} \quad (10)$$

It will be shown later through empirical evidence that  $\theta \approx i$ . Substituting this equality in equation 7 one has

$$P_n' = \tau_s a w \left[ 1 + \cos i \left( \frac{1 + \cos^2 i}{2} \right)^{1/2} - \cos i + \cot \phi_n \right] \quad (11)$$

It will be seen that equation 11 is as reliable as the more accurate equation 7 in predicting the normal force  $P_n'$ . However, when the substitution  $\theta \approx i$  was incorporated into equation 8 and checked with experimental data the errors were found to be too high.

### The Chip Flow Angle

In the following, an extension of the new model for the prediction of the chip flow angle in oblique cutting is attempted. It may be noted that such an extension to the analysis of kinematics did not form the scope of the orthogonal cutting model of Connally and Rubenstein [4].

Chip flow angle  $\rho$  has been demanding the attention of many investigators. Stabler [7] postulated that  $\rho = i$ . However, there are as many reports of deviation from this postulate as are in conformance to it. Further, the postulate does not account for the effect of rake angle, cutting conditions etc., on the chip flow angle.

In the light of the new model one way interpret  $\rho$  to be characterizing the orientation of slip near the rake surface just as  $\theta$  characterized the orientation of slip in the primary deformation zone. The velocity

$V_c$  of the chip on the rake surface can be resolved into normal ( $V_{cn}$ ) and lateral ( $V_{cl}$ ) components. Thus

$$\tan \rho = \frac{V_{cl}}{V_{cn}} \quad (12)$$

Chip velocity  $V$  is the result of successive slips along all the slip surfaces in the primary deformation zone. Only with a complete knowledge of the strain distribution on all these slip surfaces can one hope to determine the magnitudes of  $V_{cl}$  and  $V_{cn}$ . But equation 12 shows that it is necessary only to evaluate the ratio of  $V_{cl}$  to  $V_{cn}$ . If one assumes that the general orientation of slip on all the slip surfaces is same, it is enough to know the ratio of the contribution to  $V_{cl}$  and  $V_{cn}$  by any one of the slip surfaces. In other words it is being assumed that plane  $OAB$  of Fig. 1(b) characterises the orientation of slip on the slip surfaces. With this background it is now reasonable to assume that slip is 'actually' taking place only on  $S$  and  $L$ -planes for the purpose of determining  $\rho$ . Fig. 1(c) shows the ideal velocity diagram. The cutting speed  $V$  and the chip speed  $V_c$  can be resolved into normal ( $V_n$  and  $V_{cn}$ ) and lateral ( $V_l$  and  $V_{cl}$ ) components.  $V_{sn}$  and  $V_{sl}$  are the normal and lateral components of shear velocity  $V_s$  on Merchant's nominal shear plane. For the present purpose these may be distributed along  $S$  and  $L$ -planes, as shown in Fig. 1(c), and obtain the following expressions.

$$V_{sn} = \frac{V \cos \alpha_n \cos i}{\cos (\phi_n - \alpha_n)} \quad (13)$$

$$(V_{sn})_S = \frac{V_{sn} \sin \phi_n}{\sin \psi_n} \quad (14)$$

$$(V_{sn})_L = V_{sn} (\cos \phi_n - \sin \phi_n \cos \theta) \quad (15)$$

$$(V_{sl})_S = (V_{sn})_S \tan \psi_l \quad (16)$$

$$(V_{sl})_L = (V_{sn})_L \tan \theta \quad (17)$$

$$V_{cn} = \frac{V \sin \phi_n \cos i}{\cos (\phi_n - \alpha_n)} \quad (18)$$

and finally,

$$V_{cl} = V_l - V_{sl} = V \sin i - (V_{sl})_S - (V_{sl})_L \quad (19)$$

combining equations 13–19 suitably and simplifying, we have

$$\tan \rho = \tan i \sin \alpha_n + (\tan i - \tan \theta) \cos \alpha_n / \tan \phi_n \quad (20)$$

The above equation may be used either to estimate  $\rho$  from a knowledge of  $\theta$  or conversely to determine  $\theta$  from  $\rho$ . Substituting  $\rho = i$ , one may obtain the condition for Stabler's rule to be valid. It may also be noted that a substitution  $\theta = i$  leads to absurd results in equation (20). Equation 20 is very sensitive to difference  $(i - \theta)$ .

### Verification of the Model From Experimental Data

The model is now tested against oblique cutting data reported by Zorev [2], Kocecioglu [3] and Venuvinod and Lau [8] with the help of a computer. For the sake of brevity the discussion is limited to Zorev's [2] data here. However, the conclusions drawn were equally well supported by tests on the data of the other investigators. The test results on all the data are summarised in Table 1. The cutting conditions are also indicated in the table. It may be noted that the test data includes a wide range of rake angle, inclinations angle, speed and feed.

The following criteria have been used to test the accuracy of the new model:

1. In equation 7 if the coefficient of  $\tau_s$  is plotted against the measured  $P_n'$  one should get a straight line the slope of which gives the magnitude of  $\tau_s$ . The value of  $\tau_s$  so obtained should be reasonable for the given work material. It is possible to make such a plot with force  $P_n$  obtained straight from measured forces or after eliminating the parasitic force  $P_{no}$  acting at the cutting edge and the tool flank. This magnitude of  $P_{no}$  is conventionally obtained by plotting the gross force  $P_n$  against the uncut chip thickness and obtaining the intercept of the resulting straight line on the force axis.

TABLE I: SUMMARY OF RESULTS OF APPLICATION OF NEW MODEL AGAINST EXPERIMENTAL DATA

No.	Item	Zorev	Data from		Illustrated in Fig. No.
			Kocecioglu	Venuvinod and Lau	
1.	Work material	0.2% C Steel	SAE 1015, Seamless tubing 118 BHN	Al-alloy	—
2.	Tool material	HSS	HSS	HSS	—
3.	Rake angle, $\alpha_n$	20 deg	-10 to +36.5 deg	30 deg	—
4.	Inclination angle, $i$	0-60 deg	0 to 37 deg	0 to 50 deg	—
5.	Cutting speeds	0.7 m/min.	126-746 fpm	120 ipm	—
6.	Feeds	0.1-0.4 mm	0.004 to 0.012 in.	0.002 to 0.008 in.	—
7.	Range of $P_n$	120-900 kgf	120-850 lbf	120-550 lbf	2
8.	Maximum scatter of $P_n$ from equation 7	70 kgf	100 lbf	70 lbf	2
9.	Estimated $\tau_s$ from equation 7 using measured $P_n$	44 Kgf/mm <sup>2</sup>	71 $\times 10^3$ lbf/in <sup>2</sup>	20.7 $\times 10^3$ lbf/in <sup>2</sup>	2
10.	Maximum scatter of $P_n$ from Eqn. 7	60 Kgf	—	100 lbf	4
11.	Estimate of $\tau_s$ from Eqn. 7 using $P_n'$	42 Kgf/mm <sup>2</sup>	—	19.5 $\times 10^3$ lbf/in <sup>2</sup>	4
12.	Maximum scatter of $P_n$ from prediction by Merchant's Analysis	20 Kgf	120 lbf	60 lbf	3
13.	$\tau_s$ estimated by Merchant's Analysis from $P_n$	54 Kgf/mm <sup>2</sup>	69 $\times 10^3$ lbf/in <sup>2</sup>	27 $\times 10^3$ lbf/in <sup>2</sup>	3
14.	Value of C in $\theta = Ci$ from value of $P_n$	0.9	—	0.9	6
15.	Value of C in $\theta = Ci$ from values $P_n'$	0.84	—	0.85	6
16.	Maximum scatter from correlation $\theta = \theta_p$	8%	20%	—	7

2. From a given set of experimental data to obtain the value of  $\theta$  from force readings and compare the value so obtained with that determined from chip flow angle using equation 20. These two values must be close enough.

Fig. 2 shows the correlation between the predicted and actual values of  $P_n$  obtained from Zorev's data. It is seen that the agreement is good and the slope of 44 kgf/mm<sup>2</sup> is reasonable for the work material. For the sake of comparison, Fig. 3 shows the results of the same data analysed by Merchant's analysis. In this case  $P_n$  is plotted against the coefficient of  $\tau_s$  obtained by Merchant's [1] analysis. It is seen that the correlation of the new model is at least as good as Merchant's model. The slope 54 kgf/mm<sup>2</sup> in Fig. 3 is higher than the corresponding estimate of  $\tau_s$  (44 kgf/mm<sup>2</sup>) of the new model. This is understandable since in the new model the slip surface under consideration is closer to the lower boundary of shear zone than Merchant's nominal shear plane. The material has not yet work hardened.

In Fig. 4, parasitic forces have been eliminated while estimating  $P_n$

to obtain  $P_n'$  and has been compared with the estimated force from equation 7. It is seen that the general agreement is as good as in Fig. 2.

Fig. 5 illustrates the close correlation between the values of  $P_n'$  predicted with the help of equations 7 and 11. Equation 11 is found to be as good as equation 7. Equation 11 has the additional advantage that it does not need the knowledge of either  $\theta$  or the chip flow angle  $\rho$ . Such an estimation of 'p' without knowing chip flow angle is not possible from conventional shear plane analysis.

The prediction of  $P_l$  requires that the magnitude of  $\theta$  is determined first. Fig. 6 shows the variation of  $\theta$  with  $i$ , as obtained from Zorev's data. It is seen that a linear relationship between  $i$  and  $\theta$  of the following form can be obtained.

$$\theta = Ci \quad (21)$$

From Fig. 5 and Table 1 it can be concluded that the magnitude of C lies in the range 0.83 to 0.9.

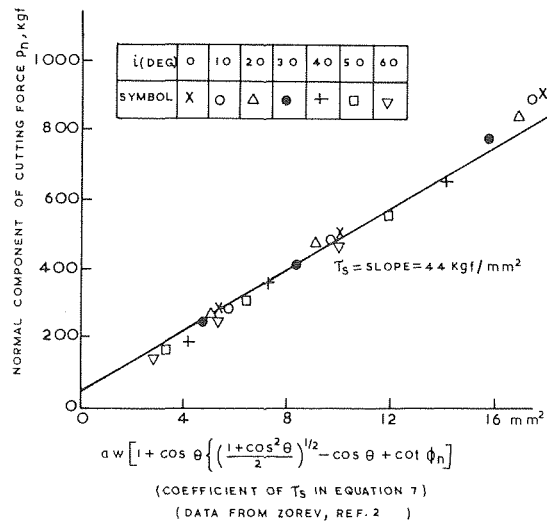


Fig. 2 Verification of equation 7 from measured forces

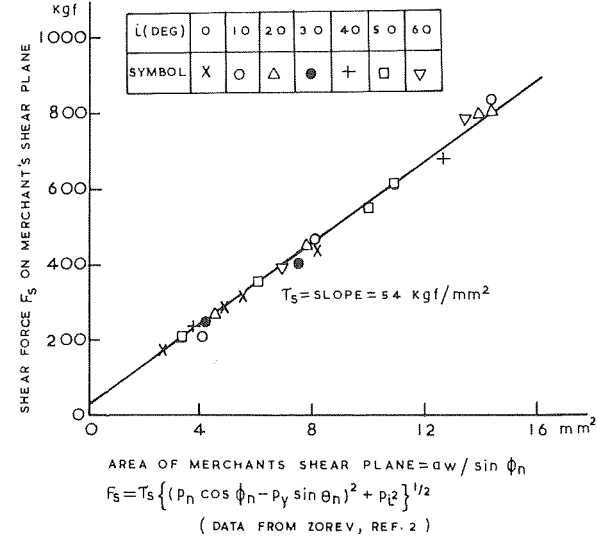


Fig. 3 Analysis of data by conventional shear plane method

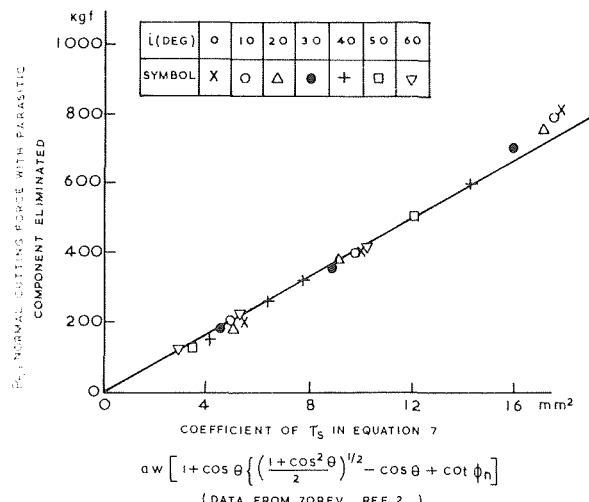


Fig. 4 Verification of equation 7 from normal forces after eliminating parasitic components

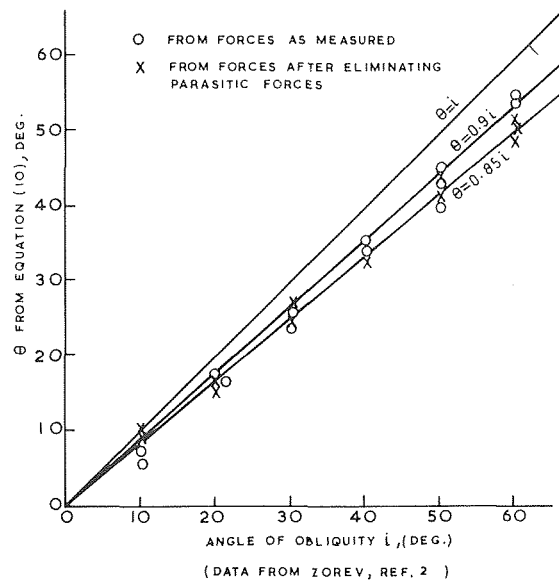


Fig. 6 Relationship between  $\theta$  and angle of obliquity

Fig. 7 compares the estimates of  $\theta$  from equation 10 based on force data and equation 20 based on chip flow angle. The agreement is remarkable. The agreement was found to be equally remarkable when the data due to Kocecioglu<sup>3</sup> and Venuvinod and Lau [8] was examined (see Table 1). This agreement is particularly impressive when it is noted that the same value of  $\theta$  is obtained from two independent sets of observations. This proves clearly the validity of the model both from the point of view of gross forces and the velocities involved. It also lends credibility to equation 20 predicting the chip flow angle. The advantage of this equation over Stabler's rule is that it includes the effect of rake and shear angles on the chip flow angle. Thus, through the shear angle, it is now possible to investigate the effects of work material and cutting conditions on chip flow angle.

In the above, the model has been looked upon as a means of predicting cutting force components. On the other hand if forces are measured, the magnitude of mean normal stress ( $p$ ) ahead of the

cutting edge can be estimated. This should be of use in any investigations regarding the effect of obliquity on phenomenon like deformation of machined surface etc. Such information would not be available if one resorted to the use of conventional shear plane analysis.

Fig. 8 is presented as yet another proof of the utility of the new model. The model is used here to analyze the data obtained during machining copper with a type II driven rotary tool of obliquity  $i = 52.5$  at different rotary speeds  $V_t$ . Here  $i_{wt}$  is a parameter characterizing the rotary speed ratio and is given by

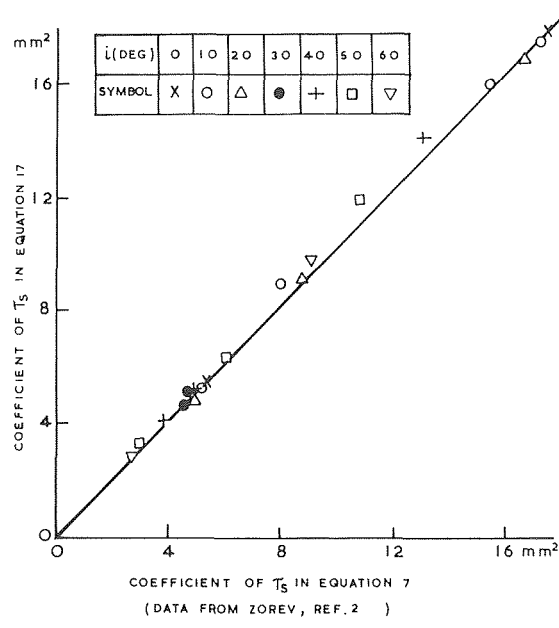


Fig. 5 Comparison of equations 7 and 11

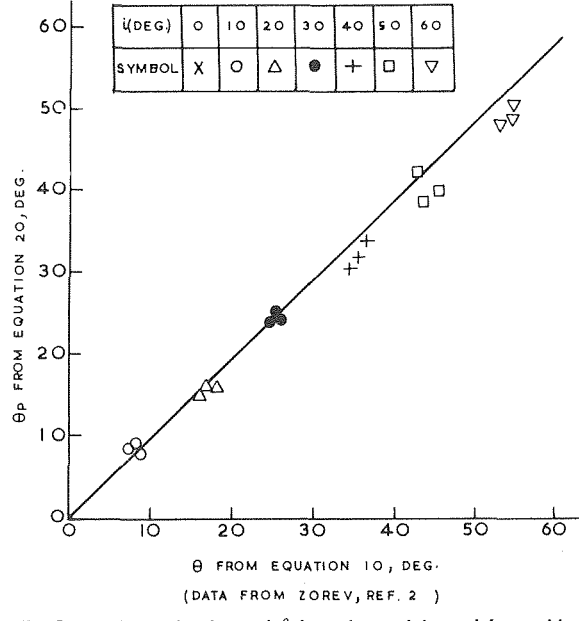


Fig. 7 Comparison of values of  $\theta$  from force data and from chip flow angle

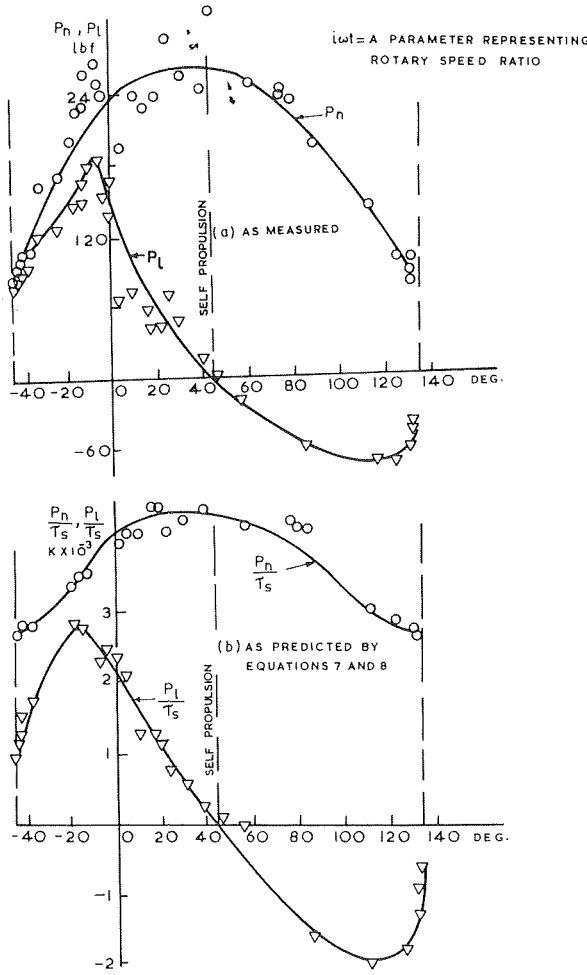


Fig. 8 Application of new model to cutting with driven rotary tools

$$\tan i_{wt} = \frac{\frac{V_t}{V} \cos i}{1 - \frac{V_t}{V} \sin i} \quad (21)$$

The chip flow angle  $\rho$  was estimated from the chip dimensions. Equation 20 was used for finding  $\theta$ . Equations 7 and 8 were used to find  $P_n/\tau_s$  and  $P_l/\tau_s$ . It is seen that agreement with measured forces

is good. The steep fall at higher values of  $i_{wt}$  is ascribed to the fall in  $\tau_s$  due to the rotary hot machining effect at higher rotary speeds.

## Conclusions

1 A new model of oblique cutting based on the pseudo slip line solution of orthogonal cutting by Connally and Rubenstein [4] has been developed. The solution has been verified against experimental data covering a wide range of cutting conditions.

2 Equation 7 or 10 may be used for the prediction of cutting force component normal to the cutting edge and lying in the cutting plane. Equation 20 may be used for the prediction of the chip flow angle,  $\theta$  a new parameter characterising the orientation of slip in the primary deformation zone, may be taken empirically to be equal to the inclination angle  $i$ .

3 The new equation for chip flow angle (equation 20) is superior to the well known Stabler's rule [7] in as much as that it includes the effect of rake and shear angles.

4 The new model is at least as effective as conventional shear plane analysis [1]. It has, however, the following additional advantages, viz:

- Prediction of normal component ( $P_n$ ) of cutting force without resort to chip flow angle; and
- estimation of the normal stress ( $p$ ) in the zone ahead of the cutting edge which is closely related to phenomenon like deformation of the machined surface etc.

## Acknowledgments

The authors thanks the University of Manchester Institute of Science and Technology, U.K., where the work was conducted, for the facilities extended. They also thank Regional Engineering College, Warangal, Andhra Pradesh (INDIA), for the help provided.

## References

- Merchant, M. E., Basic Mechanics of the Metal Cutting Process, *Journal Applied Mechanics*, No. 3, 66, 1944.
- Zorev, N. N., *Metal Cutting Mechanics*, Pergamon Press, 1966.
- Kocecioglu, D., Force Components, Chip geometry and Specific Cutting Energy in Orthogonal and oblique Machining of SAE 1015 Steel, *TRANSACTIONS ASME*, Jan. 1958, pp. 149-157.
- Connally, R., and Rubenstein, C., The Mechanics of Continuous Chip Formation in Orthogonal Cutting, *International Journal Machine Tool Design Research*, Vol. 8, 1968, pp. 159-187.
- Haslam D., and Rubenstein, C., *Annals C.I.R.P.*, 1970, Vol. 18, p. 369.
- Waishing Lau, On Work Hardening in Metal Cutting, Ph.D. thesis, University of Manchester Institute of Science and Technology, Manchester, 1971.
- Stabler, G. V., "The Fundamental Geometry of Cutting Tools," *Proceedings Institute Mechanic Engineering*, No. 63, 1951, p. 165.
- Venuvinod P. K., and Waishing Lau, On the Estimation of Chip Flow Angle in Oblique Cutting, accepted for publication in *Microtecnica*, Switzerland.
- Venuvinod, P. K., Analysis of Rotary Cutting Tools, Ph.D. thesis, University of Manchester Institute of Science and Technology, Manchester, 1971.